processes

MDPI

Article

Catalytic Hydrogenation of Nitrate over Immobilized Nanocatalysts in a Multi-Phase Continuous Reaction System: System Performance, Characterization and Optimization

Ana Sofia G. G. Santos [1,2], João Restivo [1,2], Carla Alexandra Orge [1,2], Manuel Fernando R. Pereira [1,2] and Olívia Salomé G. P. Soares [1,2,*]

[1] Laboratory of Separation and Reaction Engineering-Laboratory of Catalysis and Materials (LSRE-LCM), Faculty of Engineering, University of Porto, Rua Dr. Roberto Frias, 4200-465 Porto, Portugal; up201303231@edu.fe.up.pt (A.S.G.G.S.); jrestivo@fe.up.pt (J.R.); carlaorge@fe.up.pt (C.A.O.); fpereira@fe.up.pt (M.F.R.P.)

[2] ALiCE—Associate Laboratory in Chemical Engineering, Faculty of Engineering, University of Porto, Rua Dr. Roberto Frias, 4200-465 Porto, Portugal

* Correspondence: salome.soares@fe.up.pt

Abstract: Nitrate catalytic reduction in a continuous system was studied in the presence of Pd-Cu macrostructured catalysts synthesized through a novel washcoating methodology of the pre-formed bimetallic powder catalyst. The present work aims to understand the behavior of the macrostructured bimetallic catalyst in the presence of different reaction conditions in order to achieve the design of an optimized facility that can produce the best catalytic results: maximum NO_3^- conversion with enhanced N_2 selectivity. The residence time of the inlet solution and the catalyst concentration in the reactor proved to be the parameters that most influenced the conversion and selectivity due to the important role that these parameters play in the hydrodynamic conditions of the reactor. A higher loading of catalyst and lower inlet flow rates allow promoting a higher contact time between the three phases that participate in the reaction (G-L-S). The most efficient reaction conditions (three pieces of the macrostructured catalyst, liquid flow rate of 10 mL min^{-1}, and a total gas flow rate of 200 Ncm^3 min^{-1} (1:1 H_2:CO_2)) allowed obtaining an NO_3^- conversion of 51% with a corresponding N_2 selectivity of 23%. Also, the conversion results strongly depended on the total gas flow rate used during the reaction since this assists the mixing between the three phases and promotes a greater contact that will contribute to enhanced catalytic results.

Keywords: continuous reactor; multi-phase reaction; macrostructured catalysts; denitrification

Citation: Santos, A.S.G.G.; Restivo, J.; Orge, C.A.; Pereira, M.F.R.; Soares, O.S.G.P. Catalytic Hydrogenation of Nitrate over Immobilized Nanocatalysts in a Multi-Phase Continuous Reaction System: System Performance, Characterization and Optimization. *Processes* **2023**, *11*, 2692. https://doi.org/10.3390/pr11092692

Academic Editor: Hsin Chu

Received: 14 August 2023
Revised: 29 August 2023
Accepted: 1 September 2023
Published: 8 September 2023

1. Introduction

Nitrate (NO_3^-) is an environmental pollutant that can be commonly found in surface and groundwater. Water contamination with NO_3^- presents environmental and human health concerns related to methemoglobinemia development; several medical papers have described NO_3^- and NO_2^- as precursors for cancerous processes and thyroid malfunctions in babies and pregnant women [1–4]. Also, the carcinogenic nitrosamines may also be formed in adult stomachs upon the ingestion of nitrate-contaminated water [5,6]. The European and US legislation have established drinking water maximum concentrations of 50, 0.1, and 0.5 mg L^{-1} for NO_3^-, NO_2^-, and NH_4^+, respectively [7]. Hence, there is an increasing urgency to develop removal and control technologies for NO_3^- abatement.

Conventional water treatment systems include several methodologies to remove inorganic contaminants. However, these techniques still present some difficulties in their application [8,9]. Many procedures, such as reverse osmosis, ion exchange, and biological denitrification, have been studied over the past few years to perform NO_3^- abatement and showed efficient results for the treatment of water contaminated with NO_3^-, within the

legal limits stipulated, being techniques that are already implemented at full industrial scale [10–13]; however, disadvantages associated with high implementation costs or promotion of ion concentration without further transformation are the main disadvantages of these techniques, being imperative the study of solutions that can promote conversion into less toxic species [14].

Heterogeneous catalytic reduction allows the direct conversion of NO_3^- into less toxic species that could safely be released into the environment [15]. NO_3^- can efficiently be converted into N_2 in the presence of adequate bimetallic catalysts and a reductive agent; the main drawback is associated with the formation of NO_2^- as an intermediate by-product and excessive NH_4^+ production, which is an undesirable by-product [1,16,17]. Generally, the most accepted reaction mechanism for NO_3^- catalytic reduction was proposed by Epron et al. [18], where it is suggested that NO_3^- adsorbs on the transition metal, which is responsible for its reduction to NO_2^- through a redox reaction. Great efforts have been made, over the past few years, concerning the development of effective catalysts for NO_3^- reduction; however, their application is still limited due to NH_4^+ formation during the process [19]. The bimetallic pair Pd-Cu was demonstrated as one of the most promising for NO_3^- conversion with interesting selectivities to N_2 formation [16,19–24]. However, the efficiency of the process also depends on the reaction conditions applied during the conversion process, namely the catalyst concentration and durability (high catalytic activity without deactivation), gas flow rates, the reaction pH, and liquid flow rate (in the case of NO_3^- catalytic reduction in a continuous reactor), among other factors [1,25–27].

Several studies are reported focusing on the design and study of catalytic NO_3^- reduction in continuous systems [28–32]. One of the first studies was conducted by Pintar et al. [33], who studied the catalytic hydrogenation of NO_3^- in fixed-bed reactors, showing that NO_3^- conversion and selectivity were strongly influenced by liquid and gas flow maldistribution associated with the use of compact material beds. To avoid this type of problem, monolithic reactors emerged as interesting supports for the powder catalysts allowing immobilization of the powdered materials on structured supports and their application in heterogeneous catalytic continuous systems [34–37]. These types of structures have been widely studied over the past few years as efficient solutions to perform the catalyst immobilization for their application at the industrial level [38,39]. Also, the possibility of immobilizing powder catalysts on a structured support consists in a more sustainable approach for applying such catalysts in a catalytic water treatment system, contributing to the stability and security of the system [40,41]. However, to create an efficient system for NO_3^- conversion using a monolithic reactor, it is still required to optimize all the parameters that influence the catalytic reaction. This approach has not been adequately studied yet, since most of the studies in continuous systems are focused on fixed-bed reactors and there are very few studies on the application of monolithic reactors as support for the catalyst (macrostructured catalysts); also, most of these studies are more related to the synthesis of stable and active macrostructured catalysts and not to the optimization of reaction parameters that drive the reaction [37]. Thus, as important as the catalyst design, there is a need to understand what variables of the continuous system operation mostly contribute to the efficiency of the process using macrostructured catalysts.

The aim of the present work is the study of the catalytic liquid-phase reduction of aqueous NO_3^- solution in a continuous-flow three-phase reactor, at atmospheric pressure and room temperature, using H_2 as a reducing agent and CO_2 as a pH buffer over nanostructured catalysts immobilized on macro-structured supports. For this purpose, different inlet liquid and gas flows will be considered, as well as different H_2 and CO_2 ratios, and varying catalyst loading. It is intended to understand which would be the most important parameters to control, in order to obtain high NO_3^- conversion and selectivity to N_2, towards the up-scaling of the hydrogenation reaction of NO_3^- using a continuous reactor.

2. Materials and Methods

2.1. Bimetallic Macrostructured Catalyst Preparation

Bimetallic macrostructured catalysts were synthesized through a washcoating procedure using a pre-formed 5 wt.% Pd and 2.5 wt.% Cu powder catalyst supported on ball-milled carbon nanotubes (5%Pd–2.5%Cu/CNT(BM 2h)) [42]. The powder catalyst was synthesized by co-incipient wetness impregnation, and the synthesis procedure has been extensively described in previous works [22]. This consists of a novel methodology that allows the direct incorporation of pre-formed powder catalysts, being an interesting methodology that allows taking advantage of the mechanical modifications that are only compatible with powder material synthesis and are responsible for increasing the catalytic activity of the catalysts. This catalyst was selected for these studies considering the novelty of the process and the practicality of the synthesis methodology when compared with more conventional synthesis methods.

In the first stage, cordierite honeycomb monoliths (1 cm diameter, 6 cm length, and with 100 channels per square inch, from Corning) were thermally treated at 900 °C for 1 h in air flow to remove any impurities. A coating solution was prepared using the 5%Pd–2.5%Cu/CNT(BM 2h) powder catalyst properly dispersed in ultra-pure water by using an organic binder (Triton X-100^{TM} (TX100) from Sigma-Aldrich (St. Louis, MI, USA)). The amounts of binder and dispersant used were adjusted to maintain a 1:1 weight ratio with the powder catalyst in the slurries [43]. The monolith coating was performed 5 times, by dip-coating (30 mm min^{-1} of dipping speed and 1 min of immersion) using a Bungard RDC21 K coater, with a drying step (at 100 °C in an oven) between each coating. To perform full TX100 removal from the macrostructured catalysts structure, without compromising the catalysts activity and avoiding metal nanoparticles sintering, a washing procedure was applied to the catalyst by successive dip-coatings in a solution of isopropanol and acetone (IPA:ACN) (1:1 *v/v*) [44,45]. The resulting macrostructured catalyst was identified as a Pd-Cu/WCP_wash catalyst. An image of the macrostructured catalysts before and after coating has been added in Supplementary Information (Figure S1).

2.2. Experimental Set-Up and Procedure

Continuous catalytic experiments were performed in a custom-made experimental set-up, working in continuous mode, consisting of a bubble column with an internal recirculation loop. Figure 1 presents a schematic representation of the continuous system used during the catalytic experiments.

For the catalytic reduction experiments, an initial solution of NO_3^- (prepared from $NaNO_3$ from Sigma-Aldrich) was introduced, using a peristaltic pump, at the top of the column, at different initial NO_3^- concentrations (30, 60, and 90 mg L^{-1}). Different liquid flow rates (5, 7.5, and 10 mL min^{-1}) were studied in order to promote different residence times inside the reactor and understand how this can influence NO_3^- conversion and selectivity. The liquid flow rate of the recirculation loop is around 10 times the inlet flow rate of the system. The residence time distribution (RTD) was calculated for each of the studied liquid flow rates using a step-injection tracing method using a dye tracer. The concentration of the dye was measured at regular intervals using an UV-Vis spectrophotometer; RTD and mean residence time for each liquid flow rate were obtained by modelling the evolution of the outlet dye concentration using the Dankwertz equation applied to a continuous flow reactor [43,46]. The system presented an RTD of 20 min and took about 60 min to reach the steady state.

H_2 was used as a reducing agent and CO_2 as a pH buffer in order to maintain the solution pH value close to 5.5 (to help avoiding NH_4^+ formation). The gas was introduced at the bottom of the column, allowing the formation of a counter-current system, by using a gas diffuser. Different gas flow rates and H_2:CO_2 combinations were tested in order to optimize the conversion and selectivity. In the present work, a pre-reduction step of the catalyst was not performed; however, by the time the system reached the stationary state, it was considered that the used catalyst was pre-reduced.

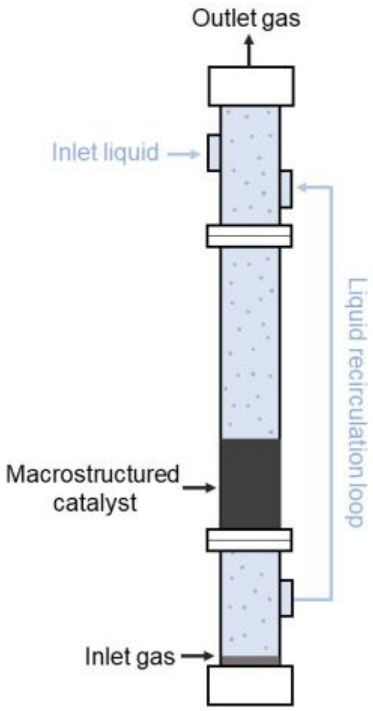

Figure 1. Reactor scheme used for the continuous NO_3^- catalytic reduction in the presence of bimetallic macrostructured catalysts.

Bubble size distribution was obtained in order to ascertain how the change in the total gas flow rate (H_2 + CO_2) could influence the bubble size distribution throughout the reaction. These experiments were performed using a focusable VLMTM2 Laser line (1.1 Mw, 635 nm 30°). The residence times were also calculated for these experiments to ascertain whether differences in the total gas flow rate could influence the liquid residence time in the column reactor.

To monitor the progress of the reaction, liquid samples were collected at the outlet of the reactor, at specific times, to quantify NO_3^-, NH_4^+, and NO_2^- concentrations. This quantification was performed by ionic chromatography in a Metrohm 881 Compact IC Pro apparatus, equipped with a Metrosep A Supp 7 Anionic Exchange Column (250 mm × 4.0 mm) for anionic species quantification and Metrosep C4 Cationic Exchange Column (250 mm × 4.0 mm) for cationic species analysis. The obtained results correspond to an average of five points taken at fixed intervals (30 min) along the reaction after the stationary state was reached. Solution pH was controlled by taking samples along the reaction time after the steady state was reached.

NO_3^- conversions and the corresponding NO_2^-, NH_4^+, and N_2 selectivities were calculated as described in [47]. The catalytic experiments performed during the present work were performed in triplicate. The maximum error registered between experiments was of 4%.

The first-order reaction rate of each experiment was calculated by application of the derived balance equation (Equation (1)). A continuous stirred-tank reactor behavior was assumed, as previously reported, due to the high ratio between the internal circulation loop and inlet flows (~10) [43]. In this equation, $C_{Steady\ state}$ corresponds to NO_3^- concentration measured at steady-state (in mg L^{-1}), and C_{Feed} represents the inlet concentration of NO_3^- that is fed to the reactor (in mg L^{-1}). k_{het} is the heterogeneous first-order reaction rate constant, and t_r represents the mean residence time in minutes (min).

$$\left[C_{Steady\ state}\right] = \frac{C_{Feed}}{1 + k_{het} \cdot t_r} \quad (1)$$

The previous equation was modified to allow a comparison between the catalytic performance of the macrostructured catalysts (Equation (2)). A deviation coefficient, d, was added to the equation representing the apparent deviation from the powder performance (which is considered as the optimal performance of the catalyst) that includes factors such as the mass transfer limitations associated with the immobilization of the catalyst on a macro-structured support and all the factors that condition the reaction kinetics in a continuous reactor [43].

$$C_{NO_3^-\,f} = \frac{C_{NO_3^-\,i}}{1 + \left(k_{NO_3^-} \cdot d_{NO_3^-}\right) \cdot t_r} \quad (2)$$

For the previous equations, $C_{NO_3^-\,i}$ represents the initial NO_3^- concentration feed to the reactor, and $C_{NO_3^-\,f}$ stands for NO_3^- concentration measured on steady-state (both in mg L^{-1}); $k_{NO_3^-}$ corresponds to the first-order reaction rate constant obtained for the corresponding powder catalyst tested in a semi-batch reactor, and t_r represents the mean residence time on the reactor (in min). An arrangement of Equation (2) allows to calculate the deviation coefficient ($d_{NO_3^-}$) associated with NO_3^- conversion, which represents the deviation associated with the reaction conditions and how these parameters influence NO_3^- conversion.

$$d_{NO_3^-} = \frac{\frac{C_{NO_3^-\,i}}{C_{NO_3^-\,f}} - 1}{k_{NO_3^-} \cdot t_r} \quad (3)$$

Another approach to this equation consisted of its arrangement considering the formation of N_2 during reaction (Equation (4)). For this specific case, $C_{N_2 f}$ corresponds to N_2 concentration after the reaction reaches the steady state, and $C_{NO_3^-\,i}$ corresponds to the initial concentration of NO_3 (both in mg L^{-1}); $k_{NO_3^-//N_2}$ represents the heterogeneous first-order reaction rate constant for N_2 formation obtained for the powder catalyst during testing in a semi-batch reactor; t_r corresponds to the residence time (in min); and $d_{NO_3^-//N_2}$ represents the deviation coefficient associated with N_2 formation. This coefficient is representative of the contribution of factors inherent to the continuous reaction process that led to the formation of N_2 during NO_3^- conversion.

$$C_{N_2 f} = C_{NO_3^-\,i} - \frac{C_{NO_3^-\,i}}{1 + \left[k_{NO_3^-//N_2} \times d_{NO_3^-//N_2}\right] \cdot t_r} \quad (4)$$

The arrangement of Equation (4) to obtain the deviation coefficient of N_2, $d_{NO_3^-//N_2}$, is present in Equation (5).

$$d_{NO_3^-//N_2} = \frac{\frac{C_{NO_3^-\,i}}{C_{NO_3^-\,i} - C_{N2_f}} - 1}{k_{NO_3^-//N_2} \cdot t_r} \quad (5)$$

Thus, $d_{NO_3^-//N_2}$ is a representative coefficient of the added interfering factors that will be in the origin of an increase or decrease of N_2 selectivity of the process.

3. Results and Discussion

3.1. Bimetallic Macrostructured Catalyst Characterization

For the present work, only one methodology was selected for the synthesis of the macro-structured catalyst, which was used throughout the study so that all the differences in performance corresponded to the influence of the operating conditions of the system.

Briefly, the catalyst presented a well-adhered carbon coating on a macro-structured cordierite support, with a carbon content of about 2% to the total mass of the macro-

structured catalyst and a metal percentage of 1.6% of Pd and 0.4% of Cu per mass of carbon present in the structure (results obtained through ICP-OES analyses). It is important to note that these percentage values obtained through ICP-OES correspond to the mass of carbon present in the catalyst, which in this case is around 200 mg for each macrostructured catalyst. TEM micrographs of this catalyst allowed us to conclude that some of the metal nanoparticles were found inside the carbon nanotubes due to a possible migration during the synthesis of the powder catalysts (before incorporation on the cordierite structure) and/or the washing methodology with an organic solvent solution applied for the removal of the surfactant from the catalyst structure, which can promote metal nanoparticles migration [44,48,49].

X-ray diffraction (XRD) results of 5%Pd–2.5%Cu/CNT(BM 2h) powder catalyst allowed to identify the formation of Pd-Cu alloys. Since the application of a washcoating procedure allowed the incorporation of this powder catalyst directly on the cordierite, these structures will also be present on the macrostructured catalyst playing a predominant role in the reaction scheme. The proximity of both metals facilitates the migration of chemisorbed H^+ and the reactants through the active centers of the catalyst, promoting a higher NO_3^- conversion degree.

SEM-EDS analysis of the structured catalyst allowed us to evaluate the metal phase distribution along the coating layer (in the cross-section), showing that the washcoating methodology results in catalysts with a homogeneous distribution of the metallic phase through the different coating layers. This distribution proved to represent a key role in the catalyst activity for NO_3^- conversion since the depth of the coating layers limits the diffusion of reactants leading to a greater difficulty for these species to contact with the catalyst active centers that are more deeply deposited. Pd-Cu/WCP_wash bimetallic catalyst was characterized in detail in previous works [42]. The used catalysts proved to be active and stable for at least 30 h of reaction.

3.2. Continuous Catalytic Experiments Results

3.2.1. Parameter Optimization Experiments

Several experiments were performed to study the influence of each parameter on the process conversion and selectivity. These studies aim not only to select the best values for each of the intervening parameters in the reaction, in order to build an active catalytic system with enhanced conversion and selectivity, but also to understand the behavior of the macrostructured bimetallic catalyst with different reaction conditions to inform the design of an optimized facility that can produce the best catalytic results. All the experiments were always performed for the same catalyst, so the obtained results correspond to the influence of the operating conditions during the reaction.

In a first stage, a blank test without the addition of a catalyst to the reaction system was performed. This experiment showed that in the absence of a catalyst, no NO_3^- conversion was registered.

Inlet NO_3^- Concentration

At this stage, different inlet NO_3^- concentrations were studied. The results obtained are presented in Figure 2.

Generally, and as it was expected, NO_3^- conversion slowly decreased with the increase of the inlet NO_3^- concentration in the feed solution of the system [50,51]. However, it is important to highlight that only a 5% decrease in activity was noticed from inlet NO_3^- concentrations of 90 mg L^{-1} to 30 mg L^{-1}, meaning that the catalyst retains its activity at much higher NO_3^- concentrations. In what concerns the process selectivities, it was possible to verify a slight increase in N_2 selectivity; however, this increase may not be directly related to the performance of the system to obtain higher N_2 conversions for higher initial NO_3^- concentrations, but with the slight loss of activity registered.

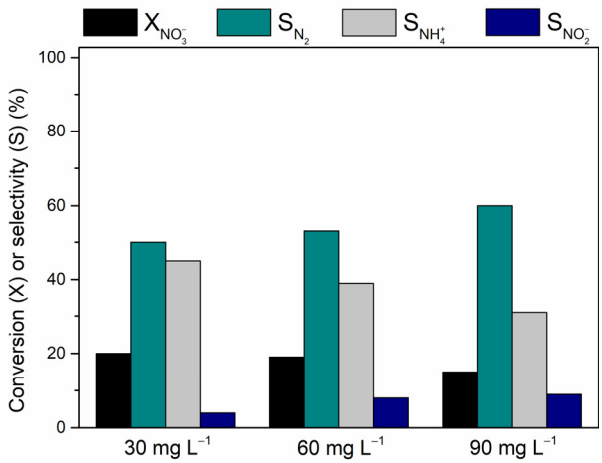

Figure 2. NO_3^- conversion and corresponding N_2, NH_4^+, and NO_2^- selectivity achieved during the experiments with different initial NO_3^- concentrations (200 Ncm^3 min^{-1} (H_2 + CO_2 (1:1) and Pd-Cu/WCP_wash catalyst).

Previous studies reported that NO_3^- initial concentrations have a significant effect on the catalytic conversion and corresponding selectivity [50–53]. No significant differences in conversion were reported for the inlet NO_3^- concentration ranges reported in the present work. In general, the largest conversion differences were reported for differences in initial NO_3^- concentrations four times higher than those tested. Such results depend on other factors, such as the properties of the reaction medium and the catalyst used. Nevertheless, it is possible to conclude that an increase in NO_3^- inlet concentration, for the same number of active centers, leads to, on the one hand, the accumulation of NO_3^- that remains unreacted due to the unavailability of Cu active centers and, on the other hand, to the accumulation of NO_2^- that is not converted due to the lack Pd active centers. This way, for this specific case, the design of the catalyst plays an important role in the conversion efficiency since the presence of more active sites will lead to a higher conversion. Also, in the case of the studied catalyst, the presence of metal alloys promotes a higher selectivity to N_2 [42].

Considering these results, and since higher conversion results were obtained for a lower NO_3^- initial concentration, 30 mg L^{-1} was selected as inlet concentration for further experiments in order to be able to further differentiate the results obtained by changing the different reaction parameters.

Liquid Flow Rates Optimization

Figure 3 presents the results obtained for NO_3^- conversion and corresponding N_2, NH_4^+, and NO_2^- selectivities, using different liquid flow rates during continuous catalytic experiments conducted with Pd-Cu/WCP_wash macrostructured catalyst.

Through the obtained results, it is possible to conclude that NO_3^- conversion substantially increases with the increase of the residence time in the reactor. This result is evident since higher residence times in the reactor allow more chances to promote the contact between NO_3^- and the catalyst [8,9,54]; however, selectivity for NH_4^+ formation was favored for lower liquid flow rates. This increase may be associated with raising the contact time between H_2 present in the liquid phase and the catalyst, which could lead to an overreduction phenomenon, which promotes a higher NH_4^+ formation. Generally, the reaction mechanism on a Pd-Cu supported catalyst starts with the adsorption of NO_3^- on Cu centers where it is going to be reduced to NO_2^- ($2Cu^0 + 2NO_3^- \rightarrow 2CuO + 2NO_2^-$) and, then, NO_2^- is desorbed from the oxidized promoter metal into the aqueous solution or directly to the reduced Pd-H_{ads} complex, where NO_2^- can be reduced to N_2 ($2NO_2^-$ + Pd-$4H_{ads} \rightarrow Pd^0 + N_2 + 4OH^-$) or NH_4^+ (NO_2^- + Pd-$6H_{ads} \rightarrow Pd^0 + NH_4^+ + 2OH^-$). The noble metal is responsible for regenerating the previously oxidized Cu center through chemisorbed hydrogen ($CuO + 2H_{ads} \rightarrow Cu^0 + H_2O$). Usually, N_2 formation is favored at an

acidic pH, while NH_4^+ formation is favored at alkaline pH. Through the equations deduced for the reaction, it is possible to verify that the presence of H_2 in large quantities can lead to an overreduction phenomenon, characterized by the presence of large amounts of reducing agent, contributing to NH_4^+ formation instead of N_2 (NO_2^- + Pd-6H_{ads} → Pd^0 + NH_4^+ + $2OH^-$ or $2NO_2^-$ + Pd-4H_{ads} → Pd^0 + N_2 + $4OH^-$). Also, it is important to highlight that changes in liquid flow will have consequences regarding the mass transfer inside macrostructured catalysts channels. This can lead to significant differences in the mixing of the three phases, which will be reflected in the conversion and selectivity values achieved.

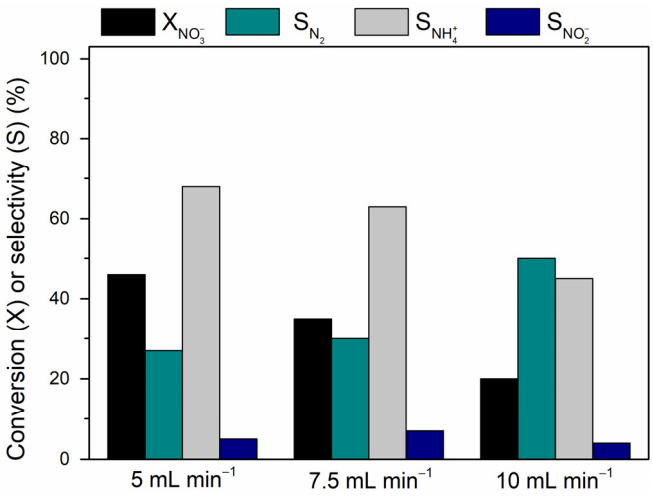

Figure 3. NO_3^- conversion and corresponding N_2, NH_4^+, and NO_2^- selectivity for different liquid flow rates ($C_{initial}[NO_3^-]$ = 30 mg L^{-1}, 200 Ncm^3 min^{-1} (H_2 + CO_2 (1:1)), and Pd-Cu/WCP_wash catalyst).

For a flow rate of 10 mL min^{-1} (corresponding to a residence time of around 20 min), it was possible to achieve an NO_3^- conversion of around 20% with a corresponding N_2 selectivity of 51%. Approximately the double of this conversion was achieved for a liquid flow rate of 5 mL min^{-1} (around 47% of NO_3^- converted); however, NH_4^+ selectivity also increased with the increasing conversion (registering selectivities of around 68% to NH_4^+ and 27% to N_2). For a liquid flow rate of 7.5 mL min^{-1} (residence time of around 28 min), an NO_3^- conversion of around 35% was registered with a corresponding N_2 selectivity of 30%.

Previous works point out the formation of higher NO_2^- concentrations for higher residence times in the reactor [27]. As reported in several papers, NO_3^- is reduced to NO_2^- on the transition metal centers of the catalyst to be further reduced to NH_4^+ or N_2 on the noble metal centers [19,25,55,56]. Thus, higher liquid flow rates, and consequently shorter residence times of the reactants inside the reactor, lead to an accumulation of by-products that did not have time to contact with the catalyst during their passage through the reactor. However, during the present work, no significant increase in NO_2^- concentration was detected when higher inlet liquid flow rates were implemented, with the large capacity of the catalyst to reduce NO_2^- being significant.

Taking into account the obtained results and the aim of the present work, it is necessary to reach a compromise between high NO_3^- conversion efficiencies and selectivity to N_2. Thus, fixing the feed liquid flow rate at 10 mL min^{-1} appears the preferred option for further optimization experiments.

Gas Flow Rates Optimization

Several experiments were performed varying H_2 and CO_2 flow rates in order to assess how the variation of these parameters would influence the conversion process and the respective selectivities for N_2 and NH_4^+ formation. Figure 4 presents the obtained results regarding NO_3^- conversion and N_2 selectivity for the different gas flow rate combinations

studied. The obtained results regarding NO_2^- and NH_4^+ selectivity were included in the Supplementary Information (Figure S2).

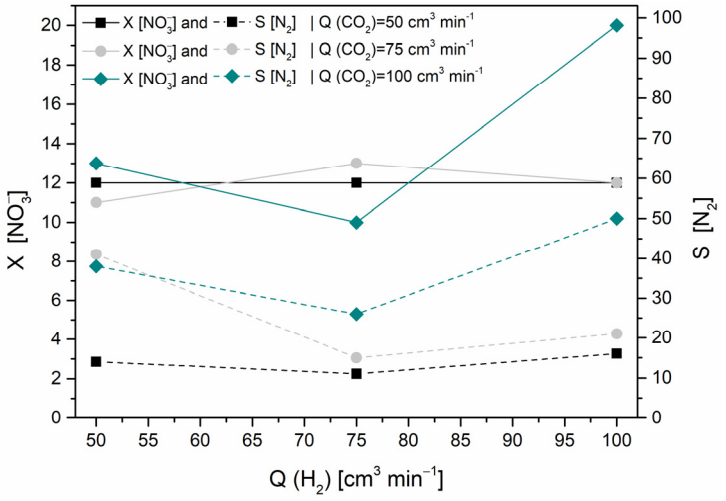

Figure 4. NO_3^- conversion and corresponding N_2 selectivity for different gas flow rate combinations ($C_{initial}[NO_3^-]$ = 30 mg L^{-1}, Q_{liquid} = 10 mL min^{-1}, and Pd-Cu/WCP_wash catalyst).

One of the most important factors to control during catalytic reduction using H_2 as a reducing agent is the flow rate at which it is fed to the reactor, which strongly influences the reduction kinetics, the conversion efficiency, and the selectivity results [25]. Generally, higher H_2 flow rates are associated with the improvement of NO_3^- conversion, and the obtained results show that NO_3^- conversion only significantly increases for an H_2 flow rate of 100 Ncm^3 min^{-1}. For lower H_2 flow rates (<100 Ncm^3 min^{-1}), the conversion results vary from 11 to 13% for all H_2:CO_2 ratios, which are not significant variations. N_2 selectivity values varied more remarkably for different H_2:CO_2 combinations. Typically, in the studies performed in the absence of the CO_2 buffer, a higher H_2 flow rate is associated with a higher NO_3^- conversion and higher NO_2^- and NH_4^+ selectivity. An increase in the H_2 flow rate provides an excess of adsorption of H_2 on the monometallic Pd sites, which may help the reaction of some of the intermediate by-products, such as NO_2^- and NO_x, with an atomic hydrogen to form N-H bonds and, this way, promote a higher NH_4^+ formation [25,27,47,56–59].

As previously mentioned, CO_2 was used as a buffer to help control the selectivity of the process by maintaining the pH of the reaction medium, which will strongly influence the selectivity of the catalytic reduction process [25]. For all the experiments using CO_2 as a buffer, the pH value was kept at values close to 5, even when using lower CO_2 flow rates. The obtained results show that N_2 selectivity increased for higher CO_2 flow rates for each of the studied H_2 flow rates. Previous studies focused on the evaluation of NO_3^- abatement in a fixed-bed reactor showed that both N_2 selectivity and the catalyst activity significantly improved when CO_2 was used to assist in pH adjustment of the reaction medium [17,25,60]. The most efficient results were obtained for a total flow rate of 200 Ncm^3 min^{-1} with a ratio of 1:1 for each gas (100 Ncm^3 min^{-1} of each gas). For this combination, an NO_3^- conversion of 20% was obtained with a corresponding N_2 selectivity of 50%.

Additional experiments were conducted without the use of CO_2 as a pH buffer, at 100 and 200 Ncm^3 min^{-1} H_2 flow rate. The latter allows direct comparison with the best performing conditions (200 Ncm^3 min^{-1} 1:1 H_2:CO_2) as the same hydrodynamic conditions are maintained. The obtained results (present in Supplementary Information) verified that the absence of CO_2 leads to a slight increase in the solution pH from 5 to 8. Generally, it was possible to verify a large NO_2^- accumulation during reaction for both experiments, although this accumulation was more evident for the experiments with higher H_2 flow rate (200 Ncm^3 min^{-1}). Also, NO_3^- conversion results were not as efficient

as in the case where CO_2 was used, showing a decrease to around 8% and 12% for the experiments with 100 Ncm^3 min^{-1} and 200 Ncm^3 min^{-1} of H_2, respectively. This was previously reported by Mendow et al. [17], who related the increase in the pH of the reaction medium with a higher conversion of NO_3^- into NO_2. The reduction of NO_3^- by itself leads to an increase in the solution pH, due to their replacement by hydroxide ions (OH^-), to keep the electroneutrality of the aqueous phase. In the absence of a pH buffer, the solution pH will increase, being responsible for negatively charging the surface of the used catalyst and, consequently, working against NO_3^- and NO_2^- adsorption due to electrostatic repulsions [15–22]. This will lead to a decrease in NO_3^- removal and an accumulation of NO_2^- in solution. Thus, it is evident, through the obtained results, that using CO_2 as a buffer plays a key role in the catalyst selectivity, allowing a good compromise between higher NO_3^- conversions (mainly achieved with high H_2 flow) while achieving higher selectivities for N_2 formation. Considering these results, the ideal ratio of 1:1 was tested for higher H_2 and CO_2 flow rates (125:125 and 150:150 Ncm^3 min^{-1}) to understand whether it would be advantageous to increase the gas flow rates. The obtained results are presented in Figure 5.

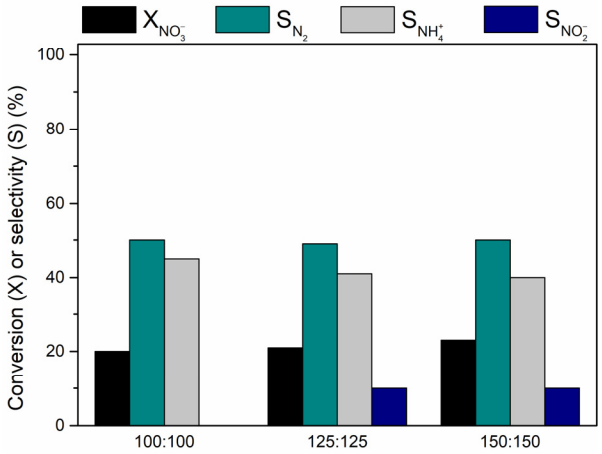

Figure 5. NO_3^- conversion and corresponding N_2, NH_4^+, and NO_2^- selectivities for higher gas flow rates ($C_{initial}[NO_3^-]$ = 30 mg L^{-1}, Q_{liquid} = 10 mL min^{-1}, and Pd-Cu/WCP_wash catalyst).

The obtained results show that there is not a significant advantage in increasing the total gas flow rate beyond 200 Ncm^3 min^{-1}, since the conversion and selectivity values remained practically unchanged, excluding the NO_2^- selectivities registered. As previously mentioned, an increase in the H_2 flow rate will result in an over-reduction phenomenon that will promote a higher NH_4^+ formation; however, the obtained results show that for higher H_2 flow rates, there is a higher accumulation of NO_2^-.

Previous studies focused on the study of the influence of gas flow rates on the residence time distribution of the reactants in the reactor show that an abrupt increase in the gas flow rate fed to the reactor could lead to significant changes in the conversion values and selectivity of the process and even lead to the accumulation of reaction by-products, as proven by the results present in Figure 5. This can happen due to a promotion of a higher recirculation of the formed vortices inside the catalyst channels that are generated by the feed of higher gas flow rates to the reactor, which can lead to an increase in the mass transfer limitations in the three-phase system and promoting the release of NO_2^- before it can react at the Pd centers to be converted to NH_4^+ or N_2 [17].

The influence of the total gas flow rate (H_2 + CO_2) fed to the reactor in the residence time of the reactants was also studied under the scope of the present work at selected total gas flow rates: 100, 200, and 300 Ncm^3 min^{-1}. The obtained results verified that there are no significant changes recorded in the residence time distributions, meaning that a sharp increase in the total gas flow rate should not cause changes in the contact time of the liquid phase reactants with the catalyst. Therefore, all changes recorded throughout

these experiments are directly related to the variation that each parameter has at the reaction level.

Coupled with these RTD tests, bubble size measurement experiments were also performed to verify if higher or smaller gas flow rates could influence the bubble size that passes through the system. Figure 6 presents the images collected during these experiments.

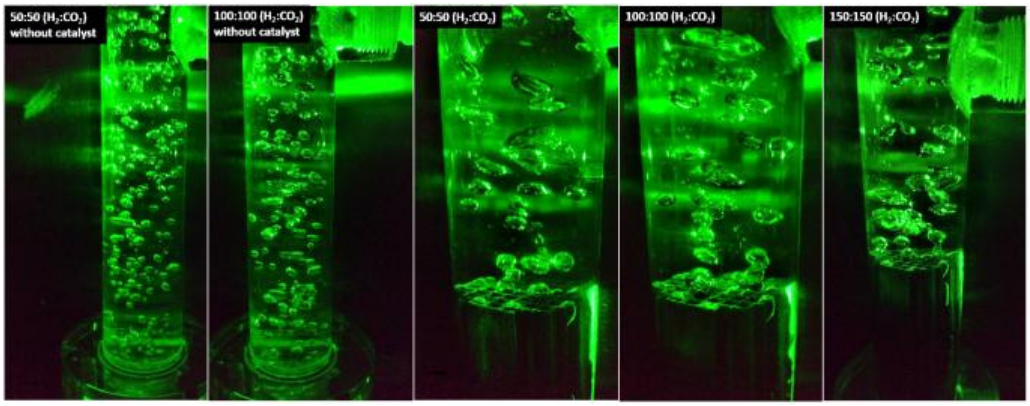

Figure 6. Images collected during bubble size experiments performed with and without catalyst in the column and for different total gas flow rates.

Generally, for blank experiments (without catalyst present in the reactor), the average bubble size remained constant (between 0.2 and 0.6 cm) for different total gas flow rates. When a catalyst is added to the column, the average bubble size, after contact with the macrostructured catalyst, increases to an average of about 1.0 to 1.5 cm. This naturally happens after gas diffusion through the channels of the macrostructured catalysts, meaning that the gas bubbles fully contact with the catalyst channels promoting the interaction between the three phases of the system (G-L-S). For this type of system, the hydrodynamic regime of interest, to promote an enhanced mass transfer, is the Taylor flow regime characterized by the formation of a segmented flow, with well-defined gas bubbles and liquid slugs crossing the channels [61–64].

Influence of the Catalyst Amount

The last step of the optimization experiments consisted of studying the influence of the catalyst amount during NO_3^- catalytic reduction. For this purpose, catalytic reduction experiments with one, two, and three pieces of catalyst in the monolithic form (all synthesized through the same methodology described in the Section 2) arranged in series in the column were performed. The obtained results are presented in Figure 7.

Typically, it is known that a higher content of catalyst results in enhanced NO_3^- conversion [25,27]. The conversion efficiency obtained with two macrostructured catalysts doubled when compared with the single catalyst reaction (20% vs. 41%). However, the process selectivity was strongly compromised with the addition of catalysts to the reaction system. N_2 selectivity decreased by half for the reaction performed with two macrostructured catalysts (from 50% registered with one catalyst to 23% registered with two catalysts). When a third catalyst was added, N_2 selectivity remained constant despite an increase in the conversion value (conversion efficiency of 51%). Previous studies reported an increase in NH_4^+ formation during reactions with higher catalyst loading [50,52,54,55]. This increase in NH_4^+ concentration may be mainly associated with the increase in the number of active sites on the catalytic system and the consequent availability of more centers for H_2 chemisorption being responsible for an over-reduction phenomenon that will promote a higher NH_4^+ formation [25].

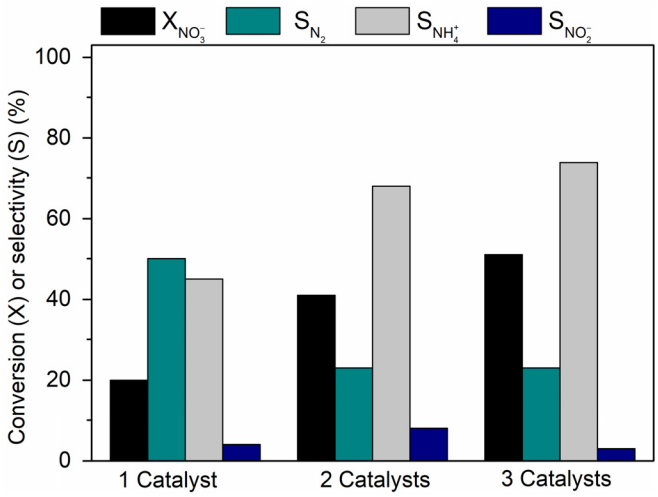

Figure 7. NO_3^- conversion and corresponding N_2, NH_4^+, and NO_2^- selectivities for the experiments with higher catalyst amount ($C_{initial}[NO_3^-]$ = 30 mg L^{-1}, Q_{liquid} = 10 mL min^{-1}, 200 Ncm^3 min^{-1} (H_2 + CO_2 (1:1)), and Pd-Cu/WCP_wash catalyst).

An important detail to note with the increase of the catalyst amount during the reaction is the decrease in NO_2^- selectivity for higher catalysts loading (from around 8% with two structured catalysts to 3% with three catalysts). This phenomenon was previously reported in other studies focused on the study of the influence of catalyst quantity, and this decrease was attributed to the existence of a greater Pd availability to perform NO_2^- reduction and, thus, resulting in a less accumulation of NO_2^- [25,27,54].

After reaction, catalysts were characterized, mainly in terms of metal leaching, which would be one of the main reasons related to the loss of activity/deactivation of the catalyst. ICP-OES analyses were performed for the liquid solutions collected after reaction. The obtained results did not show any signs of leaching of any of the metals present in the catalyst structure. In previous studies, TEM images of used bimetallic catalysts were obtained, and no significant changes in the catalyst structure were recorded, including no signs of nanoparticles sintering [22].

3.3. Assessment of Factors Affecting NO_3^- Conversion and N_2 Formation

To assess the conditioning factors that affect NO_3^- conversion and selectivities, a deviation coefficient *d* was calculated for each of the previously presented experiments. This coefficient corresponds to an apparent deviation of the results from the expected corresponding powder catalyst performance due to the characteristics of the continuous reaction system. Two different coefficients were calculated: one considering NO_3^- conversion ($d_{NO_3^-}$), in each of the previous experiments, to understand how the induced changes in the reaction system affected the conversion, and other coefficient focused on N_2 formation (d_{N_2}), which will allow evaluating how the changes in the reaction system will contribute to increase or decrease the formation of N_2, since the major goal of catalytic reaction processes is the conversion of NO_3^- into less toxic compounds (namely N_2).

These results allow performing a systematic study where it is possible to identify which of the variants has the most significant impact on the results achieved. The closer the deviation coefficient ($d_{NO_3^-}$ or d_{N_2}) value is to 1, the closer the reaction system will be to what are the ideal reaction conditions (identical to what was observed in the reactions with the powder catalyst in a stirred tank system assuming no mass transfer limitations). The obtained results are organized in different graphs grouped in Figure 8. Figure 8A–D present the results related with the deviation coefficient, considering NO_3^- conversion, as a function of each of the studied variables (inlet liquid flow rate, H_2 flow rate, CO_2 flow rate, and number of macrostructured catalysts, respectively). Figure 8E–H present the results related with the deviation coefficient, considering the selectivity to N_2, as a function of the

studied variables. Some of the results achieved with the powder catalyst tested in the batch reactor can be found in the Supplementary Information.

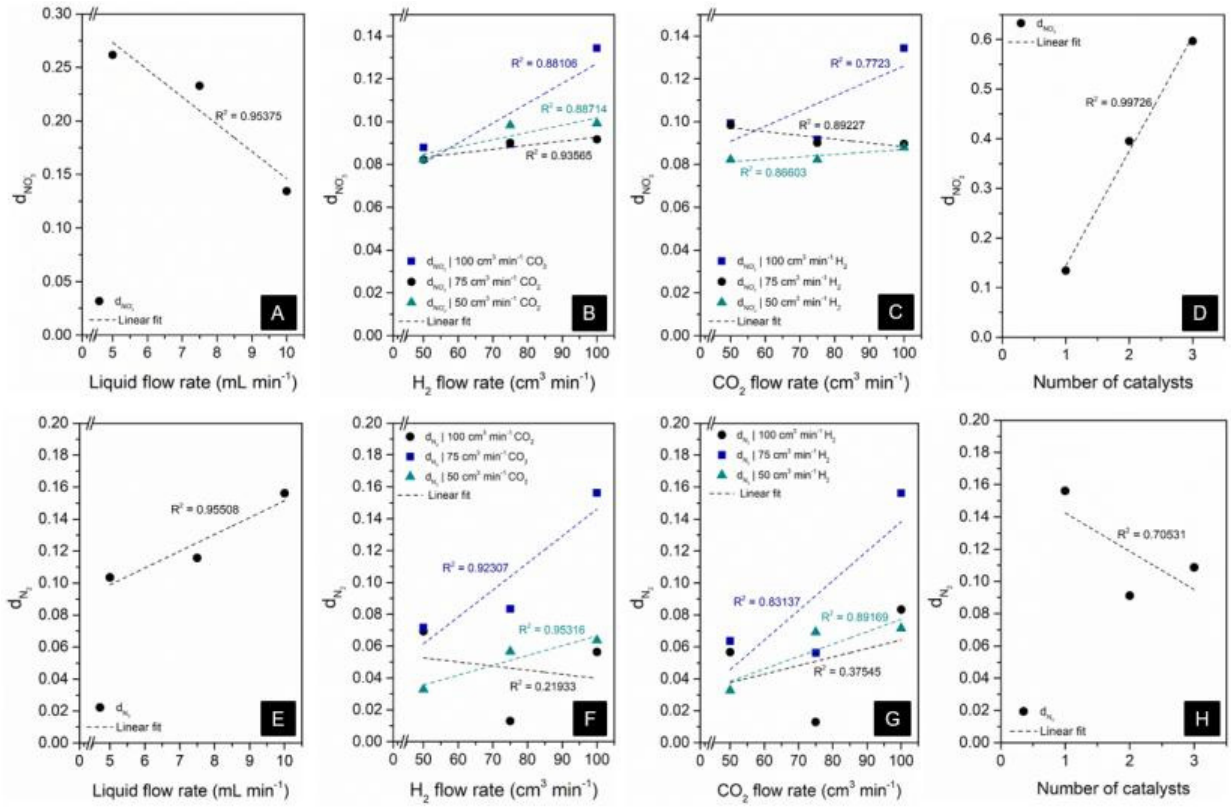

Figure 8. Fitting results for the deviation coefficient obtained for each of the reaction conditions studied: apparent deviation coefficient regarding NO_3^- conversion and N_2 selectivity obtained with different liquid flow rate (**A**,**E**), H_2 flow rate (**B**,**F**), CO_2 flow rate (**C**,**G**) and number of catalysts (**D**,**H**).

An overall analysis of the obtained results allows us to verify that the different variations in each of the parameters lead to a calculated coefficient value lower than one meaning the existence of mass transfer limitations when applying the structured catalysts in the continuous catalytic system. It is important to highlight that this coefficient, when calculated taking into account the results obtained in batch tests using the homologous catalyst in powder form, will indicate deviations from the ideal mass transfer regime (assuming no limitations) referring to external factors (such as the change of parameters in the reaction) and internal factors (related to the diffusion of reactants through the coating layer). The comparison of the deviation coefficients between each other may allow to take some conclusions regarding the system performance in different conditions (by changing the reaction parameters).

Generally, the obtained results prove that changing the flow rate of the liquid fed to the reactor and increasing the catalyst amount in the system allowed to obtain the most significant differences and the more linear correlations in terms of conversion and selectivity.

The increase of the liquid flow rate corresponds to a decrease in the residence time in the reactor and in the contact time of reactants with the solid phase catalyst, and the latter may be one of the factors that most influences the conversion and selectivity results. However, changes on the residence time of the liquid phase will have consequences on the mixing of the three phases inside the catalyst channels, causing variations that can be quite significant for the reaction system. For instance, a lower liquid flow rate will promote a higher residence time, which in turn may lead to further saturation of the liquid phase with H_2 and affect the mass transfer from the liquid and gaseous phases to the solid catalyst.

This, in turn, promotes the highest conversion of NO_3^- and greater formation of NH_4^+, due to the higher availability of H_2 in the system (results presented in Figure 8A,E).

The results corresponding to the different gas flow rates (present in Figure 8B,C,F,G) show poor linear correlations for all the combinations studied, meaning that these changes have not shown the most significant contribution to the conversion and selectivity of the process. However, the results previously presented and discussed in Figure 4 allowed to highlight an optimal combination of the two gases to obtain the maximum conversion in the studied system and the best selectivity to N_2 (100 H_2:100 CO_2 cm^3 min^{-1}). In terms of NO_3^- conversion, the variation in H_2 flow rate proved to be the most relevant factor; however, it is important to notice that, for lower H_2 flow rates (50 and 75 cm^3 min^{-1}), the deviation coefficient $d_{NO3}{}^-$ slightly increases for higher CO_2 flow rate values. These results may be related to the influence of the total gas flow rate on the hydrodynamic operation of the reactor, in particular inside the macro-structured catalyst. As previously mentioned in Section Gas Flow Rates Optimization, higher gas flow rates do not significantly impact the residence time distribution of the liquid in the reactor; however, they may significantly impact the mass transfer within the macrostructured catalyst channels. Several aspects of the Taylor flow regime inside the macrostructured catalyst channels are significantly affected by the variations in the operating conditions of the system, namely the liquid and gas flow rates. There are different parameters that are responsible for the mass transfer rate inside the structured catalyst channels, such as liquid slug length, shape, and velocity, the gas bubble length, shape, and velocity (which is conditioned by the liquid velocity), the gas hold-up, pressure drop, recirculation of the liquid and gas inside the slugs, and the film thickness between the gas bubbles and the catalyst wall [65–68]. For the specific case of the present work, the mass transfer inside the monolith channels may be promoted by a higher total gas flow rate, which is why, even for lower H_2 flow rates, there is a slight increase in NO_3^- conversion when the CO_2 flow rate increases. Higher total gas flow rates will promote a greater formation of recirculation vortexes inside the liquid slugs, promoting a higher mixture of the gas and liquid phase that will be in close contact with the catalyst channels. A similar effect is seen with changing liquid flow rates, affecting the formation of the liquid slug vortices inside the catalyst, and hence the changes in the corresponding $d_{NO3}{}^-$. Previous studies have reported that the decrease on the liquid velocity inside the monolith channels would enhance the mass transference through the thin film of liquid joining the three phases participating in the reaction (G-L-S) since this film becomes thinner [69]. In what concerns to the gas to liquid mass transfer (G-L), previous studies reported that this is not necessarily a function of the bubble length but will strongly depend on the liquid slug length, and typically the thinner the slug length, the higher the mass transference between both phases and, consequently, between the third phase involved in the reaction (as previously mentioned) [69].

Higher CO_2 flow rates proved to have a more significant impact on the decrease of undesirable by-product formation (Figure 8G).

The amount of catalyst present in the reactor seems to be one of the most relevant factors to improve NO_3^- catalytic conversion (Figure 8D); however, it was revealed to be quite detrimental regarding the formation of sub-products, mainly NH_4^+ formation (Figures 7 and 8H). It is evident that a higher amount of catalyst will positively contribute to the reaction extent since it adds active centers to the system where the reaction can occur. On the other hand, as more catalysts are added to the system, the contact time of the reactants with the catalyst increases. Figure 9 presents the results obtained for the deviation coefficient considering the contact time with the catalyst, instead of the residence time in the reactor in Equation (3) (t_r).

As previously discussed, the main factor influencing the increase of NO_3^- conversion in a continuous process using macrostructured catalysts is the intimate contact between the three phases involved in the reaction. Thus, increasing the contact time between reactants and solid catalysts by adding three pieces of the catalyst in the monolithic form to the system (maximum held by the reactor) should result in a linear increase in $d_{NO3}{}^-$. However, the

deviation coefficient only significantly increased for the experiment with two monoliths in the reactor, whereas when the third monolith was added, the coefficient remained constant. On one hand, it would be possible that the increase in the number of active centers was not contributing to the reaction kinetics after a certain amount. However, the linear increase in Figure 8D suggests otherwise. Thus, this is likely related to the formation of larger gas bubbles after the first monolith in series, since the process of formation of these bubbles is then not present between the second and third monoliths, which in turn affects the mass transfer between phases inside the monoliths by altering the hydrodynamic regime.

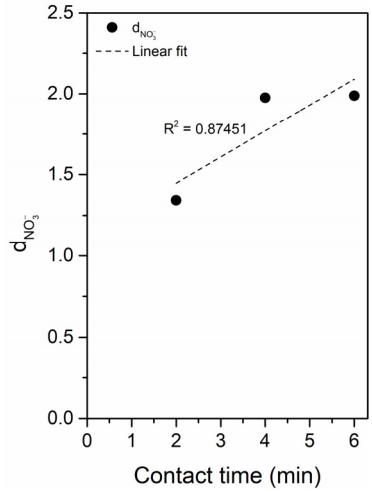

Figure 9. Fitting results for the deviation coefficient obtained for NO_3^- conversion considering the contact time with the macrostructured catalyst.

3.4. Final Remarks

The results previously presented allow to conclude that there is a significant influence of the reaction conditions on the hydrodynamic behavior of the reactor. Generally, there is an ideal liquid and total gas flow rate, which results in the most promising NO_3^- conversion and N_2 selectivity results. The reaction conditions that have a higher influence on the catalytic results are those with a more significant impact on the residence time of the pollutants inside the reactor and that promote an extensive contact between the three phases (three monoliths, liquid flow rate of 10 mL min^{-1}, and a total gas flow rate of 200 Ncm^3 min^{-1} (1:1 H_2:CO_2)). The obtained results indicate that there are no significant changes in the selectivity when varying the reaction conditions. Thus, the system is optimized to obtain results that allow the best compromise between obtaining an efficient NO_3^- conversion and good selectivity to N_2 formation. Therefore, the current system would only be efficient (and optimizable) in a specific range of conditions that would allow conversion of nitrate below the 50 mg L^{-1} limit while maintaining NH_4^+ concentration below the legal limit. Nevertheless, it is also evident that there are still further opportunities to improve selectivity to N_2 by optimizing the catalysts' formulation by controlling the formation of structures that would promote its formation during reaction. As it was previously shown with the obtained results, one of the parameters that most influenced the catalytic results obtained with the designed continuous catalytic system was the catalyst concentration inside the reactor; this is an additional parameter where there must be additional optimization either in the amount of powder catalyst possible to incorporate in the macroscopic structure, or by the availability of active centers to participate in reaction. At this point, in the present work, an optimized continuous catalytic system to be implemented for NO_3^- conversion is presented; however, additional studies need to be performed (mainly concerning catalyst design) in order to implement this type of system at a full scale.

4. Conclusions

The present work aims to study and optimize the reaction conditions applied in a continuous catalytic system for the selective conversion of NO_3^- to N_2. Several factors, such as the liquid flow rate fed to the system, the gas flow rate, the combination of both gases (H_2 and CO_2), and the amount of catalyst present in the reaction, strongly condition the conversion process and the respective selectivity. Therefore, this work allowed identifying how these factors interfere in the reaction system and, in this way, perform its optimization towards the best compromise between an efficient NO_3^- conversion and good selectivity for the formation of less toxic by-products (N_2).

Generally, the inlet liquid flow rate and the catalyst amount inside the reactor were the parameters that most influenced the conversion and selectivities due to the important role these parameters play in defining the hydrodynamic conditions of the reactor. Higher loading of catalyst (higher number of macrostructured catalysts in the reactor) promoted higher contact time between the three phases (G-L-S), leading to more efficient conversion results; however, N_2 selectivity was somewhat compromised during these experiments. In this case, the optimization of gas flow rate and the ratio of both gases play a major role in the selectivity control. In addition, the optimized gas flow rate and ratio also correspond to the best conditions that promote a higher mixture of gas and liquid phases inside the macrostructured catalyst channels, thus promoting greater contact between the three phases. The most efficient gas combination was a total gas flow rate of 200 Ncm^3 min^{-1} (1:1 of each gas), which proved to be preponderant in promoting a greater mixture of the various phases involved in the reaction.

This way, the developed work allowed us to study, in detail, the factors that most contribute to the efficiency of the reaction conditions, allowing its optimization to achieve a more efficient catalytic system for selective NO_3^- conversion.

Supplementary Materials: The following supporting information can be downloaded at: https://www.mdpi.com/article/10.3390/pr11092692/s1.

Author Contributions: Conceptualization, J.R., C.A.O. and O.S.G.P.S.; investigation, A.S.G.G.S. and J.R.; resources, M.F.R.P. and O.S.G.P.S.; writing—original draft preparation, A.S.G.G.S.; writing—review and editing, J.R., C.A.O., M.F.R.P. and O.S.G.P.S.; supervision, C.A.O., O.S.G.P.S. and M.F.R.P.; funding acquisition, C.A.O., M.F.R.P. and O.S.G.P.S. All authors have read and agreed to the published version of the manuscript.

Funding: This research was financially supported by NanoCatRed (NORTE-01-0247-FEDER-045925), co-financed by the ERDF—European Regional Development Fund, through the Operation Program for Competitiveness and Internationalization—COMPETE 2020, the North Portugal Regional Operational Program—NORTE 2020, and by the Portuguese Foundation for Science and Technology—FCT under UT Austin Portugal; LA/P/0045/2020 (ALiCE), UIDB/50020/2020, and UIDP/50020/2020 (LSRE-LCM), funded by national funds through FCT/MCTES (PIDDAC). C.A.O. acknowledges FCT funding under the DL57/2016 Transitory Norm Program. O.S.G.P.S. acknowledges FCT funding under the Scientific Employment Stimulus—Institutional Call CEECINST/00049/2018.

Data Availability Statement: The data presented in this study are available on request from the corresponding author.

Conflicts of Interest: The authors declare no conflict of interest.

References

1. Prüsse, U.; Hähnlein, M.; Daum, J.; Vorlop, K.-D. Improving the catalytic nitrate reduction. *Catal. Today* **2000**, *55*, 79–90. [CrossRef]
2. Gatseva, P.D.; Argirova, M.D. High-nitrate levels in drinking water may be a risk factor for thyroid dysfunction in children and pregnant women living in rural Bulgarian areas. *Int. J. Hyg. Environ. Health* **2008**, *211*, 555–559. [CrossRef]
3. Fraser, P.; Chilvers, C. Health aspects of nitrate in drinking water. *Sci. Total Environ.* **1981**, *18*, 103–116. [CrossRef] [PubMed]
4. Winton, E.F.; Tardiff, R.G.; McCabe, L.J. Nitrate in drinking water. *J.-Am. Water Work. Assoc.* **1971**, *63*, 95–98. [CrossRef]
5. Menció, A.; Mas-Pla, J.; Otero, N.; Regàs, O.; Boy-Roura, M.; Puig, R.; Bach, J.; Domènech, C.; Zamorano, M.; Brusi, D. Nitrate pollution of groundwater all right. . ., but nothing else? *Sci. Total Environ.* **2016**, *539*, 241–251. [CrossRef]

6. Yang, C.; Cheng, M.; Tsai, S.; Hsieh, Y. Calcium, magnesium, and nitrate in drinking water and gastric cancer mortality. *Jpn. J. Cancer Res.* **1998**, *89*, 124–130. [CrossRef]
7. Barrabés, N.; Sá, J. Catalytic nitrate removal from water, past, present and future perspectives. *Appl. Catal. B Environ.* **2011**, *104*, 1–5. [CrossRef]
8. Zhou, M.; Wang, W.; Chi, M. Enhancement on the simultaneous removal of nitrate and organic pollutants from groundwater by a three-dimensional bio-electrochemical reactor. *Bioresour. Technol.* **2009**, *100*, 4662–4668. [CrossRef]
9. Moussavi, G.; Shekoohiyan, S. Simultaneous nitrate reduction and acetaminophen oxidation using the continuous-flow chemical-less VUV process as an integrated advanced oxidation and reduction process. *J. Hazard. Mater.* **2016**, *318*, 329–338. [CrossRef]
10. Pintar, A.; Batista, J.; Levec, J. Catalytic denitrification: Direct and indirect removal of nitrates from potable water. *Catal. Today* **2001**, *66*, 503–510. [CrossRef]
11. Yang, T.; Doudrick, K.; Westerhoff, P. Photocatalytic reduction of nitrate using titanium dioxide for regeneration of ion exchange brine. *Water Res.* **2013**, *47*, 1299–1307. [CrossRef] [PubMed]
12. Anoop, K.; Viraraghavan, T. Nitrate Removal From Drinking Water—Review. *J. Environ. Eng.* **1997**, *123*, 371–380. [CrossRef]
13. Jensen, V.B.; Darby, J.L.; Seidel, C.; Gorman, C.; Jensen, V.B.; Darby, J.L.; Seidel, C.; Gorman, C.; Gorman, C. Nitrate in Potable Water Supplies: Alternative Management Strategies. *Crit. Rev. Environ. Sci. Technol.* **2014**, *44*, 2203–2286. [CrossRef]
14. Mendow, G.; Veizaga, N.S.; Querini, C.A.; Sánchez, B.S. A continuous process for the catalytic reduction of water nitrate. *J. Environ. Chem. Eng.* **2019**, *7*, 102808. [CrossRef]
15. Prüsse, U.; Vorlop, K.-D. Supported bimetallic palladium catalysts for water-phase nitrate reduction. *J. Mol. Catal. A Chem.* **2001**, *173*, 313–328. [CrossRef]
16. Gauthard, F.; Epron, F.; Barbier, J. Palladium and platinum-based catalysts in the catalytic reduction of nitrate in water: Effect of copper, silver, or gold addition. *J. Catal.* **2003**, *220*, 182–191. [CrossRef]
17. Mendow, G.; Marchesini, F.A.; Miro, E.E.; Querini, C.A. Evaluation of Pd- In supported catalysts for water nitrate abatement in a fixed-bed continuous reactor. *Ind. Eng. Chem. Res.* **2011**, *50*, 1911–1920. [CrossRef]
18. Epron, F.; Gauthard, F.; Pinéda, C.; Barbier, J. Catalytic reduction of nitrate and nitrite on Pt–Cu/Al2O3 catalysts in aqueous solution: Role of the interaction between copper and platinum in the reaction. *J. Catal.* **2001**, *198*, 309–318. [CrossRef]
19. Hörold, S.; Vorlop, K.-D.; Tacke, T.; Sell, M. Development of catalysts for a selective nitrate and nitrite removal from drinking water. *Catal. Today* **1993**, *17*, 21–30. [CrossRef]
20. Lubphoo, Y.; Chyan, J.-M.; Grisdanurak, N.; Liao, C.-H. Nitrogen gas selectivity enhancement on nitrate denitrification using nanoscale zero-valent iron supported palladium/copper catalysts. *J. Taiwan Inst. Chem. Eng.* **2015**, *57*, 143–153. [CrossRef]
21. Pintar, A.; Batista, J.; Muševič, I. Palladium-copper and palladium-tin catalysts in the liquid phase nitrate hydrogenation in a batch-recycle reactor. *Appl. Catal. B Environ.* **2004**, *52*, 49–60. [CrossRef]
22. Santos, A.; Restivo, J.; Orge, C.A.; Pereira, M.F.R.; Soares, O. Nitrate Catalytic Reduction over Bimetallic Catalysts: Catalyst Optimization. *C* **2020**, *6*, 78. [CrossRef]
23. Soares, O.S.G.P.; Órfão, J.J.M.; Pereira, M.F.R. Nitrate Reduction Catalyzed by Pd–Cu and Pt–Cu Supported on Different Carbon Materials. *Catal. Lett.* **2010**, *139*, 97–104. [CrossRef]
24. Sá, J.; Gross, S.; Vinek, H. Effect of the reducing step on the properties of Pd-Cu bimetallic catalysts used for denitration. *Appl. Catal. A Gen.* **2005**, *294*, 226–234. [CrossRef]
25. Tokazhanov, G.; Ramazanova, E.; Hamid, S.; Bae, S.; Lee, W. Advances in the catalytic reduction of nitrate by metallic catalysts for high efficiency and N2 selectivity: A review. *Chem. Eng. J.* **2020**, *384*, 123252. [CrossRef]
26. Hu, M.; Liu, Y.; Yao, Z.; Ma, L.; Wang, X. Catalytic reduction for water treatment. *Front. Environ. Sci. Eng.* **2017**, *12*, 3. [CrossRef]
27. Chen, Y.-X.; Zhang, Y.; Chen, G.-H. Appropriate conditions or maximizing catalytic reduction efficiency of nitrate into nitrogen gas in groundwater. *Water Res.* **2003**, *37*, 2489–2495. [CrossRef]
28. Barrabés, N.; Just, J.; Dafinov, A.; Medina, F.; Fierro, J.L.G.; Sueiras, J.E.; Salagre, P.; Cesteros, Y. Catalytic reduction of nitrate on Pt-Cu and Pd-Cu on active carbon using continuous reactor: The effect of copper nanoparticles. *Appl. Catal. B Environ.* **2006**, *62*, 77–85. [CrossRef]
29. Shukla, A.; Pande, J.V.; Bansiwal, A.; Osiceanu, P.; Biniwale, R.B. Catalytic Hydrogenation of Aqueous Phase Nitrate Over Fe/C Catalysts. *Catal. Lett.* **2009**, *131*, 451–457. [CrossRef]
30. Marchesini, F.A.; Mendow, G.; Picard, N.P.; Zoppas, F.M.; Aghemo, V.S.; Gutierrez, L.B.; Querini, C.A.; Miro, E.E. PdIn catalysts in a continuous fixed bed reactor for the nitrate removal from groundwater. *Int. J. Chem. React. Eng.* **2019**, *17*, 20180126. [CrossRef]
31. Barrabés, N.; Dafinov, A.; Medina, F.; Sueiras, J.E. Catalytic reduction of nitrates using Pt/CeO2 catalysts in a continuous reactor. *Catal. Today* **2010**, *149*, 341–347. [CrossRef]
32. Aristizábal, A.; Contreras, S.; Barrabés, N.; Llorca, J.; Tichit, D.; Medina, F. Catalytic reduction of nitrates in water on Pt promoted Cu hydrotalcite-derived catalysts: Effect of the Pt–Cu alloy formation. *Appl. Catal. B Environ.* **2011**, *110*, 58–70. [CrossRef]
33. Pintar, A.; Batista, J. Catalytic hydrogenation of aqueous nitrate solutions in fixed-bed reactors. *Catal. Today* **1999**, *53*, 35–50. [CrossRef]
34. Yuranova, T.; Kiwi-Minsker, L.; Franch, C.; Palomares, A.E.; Armenise, S.; García-Bordejé, E. Nanostructured catalysts for the continuous reduction of nitrates and bromates in water. *Ind. Eng. Chem. Res.* **2013**, *52*, 13930–13937. [CrossRef]
35. Restivo, J.; Soares, O.; Orfao, J.J.M.; Pereira, M.F.R. Catalytic reduction of bromate over monometallic catalysts on different powder and structured supports. *Chem. Eng. J.* **2017**, *309*, 197–205. [CrossRef]

36. Wa, J.; Turunen, I.; Salmi, T.; Maunula, T. Kinetics of nitrate reduction in monolith reactor. *Chem. Eng. Sci.* **1994**, *49*, 5763–5773. [CrossRef]
37. Peroni, B.; Navas, M.; Bideberripe, H.P.; Barbero, B.; Casella, M.L.; Jaworski, M.A. Development of PdCu Structured Catalysts Based on ZrO2–CeO2 Materials Supported on Cordierite Monoliths for Water Remediation: Removal of Hazardous Oxyanions. *Ind. Eng. Chem. Res.* **2021**, *60*, 12767–12775. [CrossRef]
38. Hosseini, S.; Moghaddas, H.; Masoudi Soltani, S.; Kheawhom, S. Technological Applications of Honeycomb Monoliths in Environmental Processes: A review. *Process Saf. Environ. Prot.* **2020**, *133*, 286–300. [CrossRef]
39. Ren, Z.; Guo, Y.; Gao, P.-X. Nano-array based monolithic catalysts: Concept, rational materials design and tunable catalytic performance. *Catal. Today* **2015**, *258*, 441–453. [CrossRef]
40. Tomašić, V.; Jović, F. State-of-the-art in the monolithic catalysts/reactors. *Appl. Catal. A Gen.* **2006**, *311*, 112–121. [CrossRef]
41. Cybulski, A.; Moulijn, J.A. Monoliths in Heterogeneous Catalysis. *Catal. Rev.* **1994**, *36*, 179–270. [CrossRef]
42. Santos, A.S.G.G.; Restivo, J.; Orge, C.A.; Pereira, M.F.R.; Soares, O.S.G.P. Design of macrostructured bimetallic MWCNT catalysts for multi-phasic hydrogenation in water treatment with pre- and post-coating metal phase impregnation. *Appl. Catal. A Gen.* **2022**, *643*, 118790. [CrossRef]
43. Restivo, J.; Orge, C.A.; Guedes Gorito dos Santos, A.S.; Gonçalves Pinto Soares, O.S.; Ribeiro Pereira, M.F. Influence of preparation methods on the activity of macro-structured ball-milled MWCNT catalysts in the ozonation of organic pollutants. *J. Environ. Chem. Eng.* **2020**, 104578. [CrossRef]
44. Rojas, J.A.; Ardila-Rodríguez, L.A.; Diniz, M.F.; Gonçalves, M.; Ribeiro, B.; Rezende, M.C. Optimization of Triton X-100 removal and ultrasound probe parameters in the preparation of multiwalled carbon nanotube buckypaper. *Mater. Des.* **2019**, *166*, 107612. [CrossRef]
45. Santos, A.; Restivo, J.; Orge, C.A.; Pereira, M.F.R.; Soares, O. Synthesis of monometallic macrostructured catalysts for bromate reduction in a continuous catalytic system. *Environ. Technol.* **2022**. [CrossRef]
46. Nauman, E.B. *Residence Time Distributions*; Wiley: Hoboken, NJ, USA, 2003.
47. Soares, O.S.G.; Fan, X.; Orfao, J.J.; Lapkin, A.A.; Pereira, M.F.R. Kinetic Modeling of Nitrate Reduction Catalyzed by Pd-Cu Supported on Carbon Nanotubes. *Ind. Eng. Chem. Res.* **2012**, *51*, 4854–4860. [CrossRef]
48. Panić, S.; Kukovecz, Á.; Boskovic, G. Design of catalytic carbon nanotube-based reactor for water denitration—The impact of active metal confinement. *Appl. Catal. B Environ.* **2018**, *225*, 207–217. [CrossRef]
49. Soares, O.S.G.P.; Gonçalves, A.G.; Delgado, J.J.; Órfão, J.J.M.; Pereira, M.F.R. Modification of carbon nanotubes by ball-milling to be used as ozonation catalysts. *Catal. Today* **2015**, *249*, 199–203. [CrossRef]
50. Hamid, S.; Lee, W. Nitrate reduction by iron supported bimetallic catalyst in low and high nitrogen regimes. *Adv. Environ. Res.* **2015**, *4*, 263–271. [CrossRef]
51. Huang, C.-P.; Wang, H.-W.; Chiu, P.-C. Nitrate reduction by metallic iron. *Water Res.* **1998**, *32*, 2257–2264. [CrossRef]
52. Liu, H.; Guo, M.; Zhang, Y. Nitrate removal by Fe0/Pd/Cu nano-composite in groundwater. *Environ. Technol.* **2014**, *35*, 917–924. [CrossRef]
53. Zhang, Y.; Douglas, G.B.; Pu, L.; Zhao, Q.; Tang, Y.; Xu, W.; Luo, B.; Hong, W.; Cui, L.; Ye, Z. Zero-valent iron-facilitated reduction of nitrate: Chemical kinetics and reaction pathways. *Sci. Total Environ.* **2017**, *598*, 1140–1150. [CrossRef] [PubMed]
54. Hamid, S.; Bae, S.; Lee, W.; Amin, M.T.; Alazba, A.A. Catalytic nitrate removal in continuous bimetallic Cu–Pd/nanoscale zerovalent iron system. *Ind. Eng. Chem. Res.* **2015**, *54*, 6247–6257. [CrossRef]
55. Vorlop, K.-D.; Tacke, T. Erste schritte auf dem weg zur edelmetallkatalysierten nitrat-und nitrit-entfernung aus trinkwasser. *Chemieingenieurtechnik* **1989**, *61*, 836–837. [CrossRef]
56. Hamid, S.; Bae, S.; Lee, W. Novel bimetallic catalyst supported by red mud for enhanced nitrate reduction. *Chem. Eng. J.* **2018**, *348*, 877–887. [CrossRef]
57. Strukul, G.; Gavagnin, R.; Pinna, F.; Modaferri, E.; Perathoner, S.; Centi, G.; Marella, M.; Tomaselli, M. Use of palladium based catalysts in the hydrogenation of nitrates in drinking water: From powders to membranes. *Catal. Today* **2000**, *55*, 139–149. [CrossRef]
58. Jung, J.; Bae, S.; Lee, W. Nitrate reduction by maghemite supported Cu-Pd bimetallic catalyst. *Appl. Catal. B Environ.* **2012**, *127*, 148–158. [CrossRef]
59. Zhao, W.; Zhu, X.; Wang, Y.; Ai, Z.; Zhao, D. Catalytic reduction of aqueous nitrates by metal supported catalysts on Al particles. *Chem. Eng. J.* **2014**, *254*, 410–417. [CrossRef]
60. D'Arino, M.; Pinna, F.; Strukul, G. Nitrate and nitrite hydrogenation with Pd and Pt/SnO2 catalysts: The effect of the support porosity and the role of carbon dioxide in the control of selectivity. *Appl. Catal. B Environ.* **2004**, *53*, 161–168. [CrossRef]
61. Nijhuis, T.A.; Kreutzer, M.T.; Romijn, A.C.J.; Kapteijn, F.; Moulijn, J.A. Monolithic catalysts as more efficient three-phase reactors. *Catal. Today* **2001**, *66*, 157–165. [CrossRef]
62. Roy, S.; Bauer, T.; Al-Dahhan, M.; Lehner, P.; Turek, T. Monoliths as multiphase reactors: A review. *AIChE J.* **2004**, *50*, 2918–2938. [CrossRef]
63. Roy, S.; Al-Dahhan, M. Flow distribution characteristics of a gas–liquid monolith reactor. *Catal. Today* **2005**, *105*, 396–400. [CrossRef]
64. Heiszwolf, J.J.; Kreutzer, M.T.; van den Eijnden, M.G.; Kapteijn, F.; Moulijn, J.A. Gas–liquid mass transfer of aqueous Taylor flow in monoliths. *Catal. Today* **2001**, *69*, 51–55. [CrossRef]

65. Ito, D.; Damsohn, M.; Prasser, H.-M.; Aritomi, M. Dynamic film thickness between bubbles and wall in a narrow channel. *Exp. Fluids* **2011**, *51*, 821–833. [CrossRef]
66. Tsoligkas, A.N.; Simmons, M.J.H.; Wood, J.; Frost, C.G. Kinetic and selectivity studies of gas–liquid reaction under Taylor flow in a circular capillary. *Catal. Today* **2007**, *128*, 36–46. [CrossRef]
67. Bercic, G.; Pintar, A. The role of gas bubbles and liquid slug lengths on mass transport in the Taylor flow through capillaries. *Chem. Eng. Sci.* **1997**, *52*, 3709–3719. [CrossRef]
68. Vandu, C.O.; Ellenberger, J.; Krishna, R. Hydrodynamics and mass transfer in an upflow monolith loop reactor. *Chem. Eng. Process. Process Intensif.* **2005**, *44*, 363–374. [CrossRef]
69. Kreutzer, M.T.; Du, P.; Heiszwolf, J.J.; Kapteijn, F.; Moulijn, J.A. Mass transfer characteristics of three-phase monolith reactors. *Chem. Eng. Sci.* **2001**, *56*, 6015–6023. [CrossRef]